PHYSICAL REVIEW B
CONDENSED MATTER

THIRD SERIES, VOLUME 35, NUMBER 15 15 MAY 1987-II

Surface waves in Au/Cr superlattices

P. Bisanti,* M. B. Brodsky, G. P. Felcher, M. Grimsditch, and L. R. Sill†
Materials Science Division, Argonne National Laboratory, Argonne, Illinois 60439
(Received 3 November 1986)

The results of x-ray and Brillouin scattering experiments on Au/Cr superlattices are presented. X-ray diffraction results indicate dramatic changes in the lattice parameters of Au and Cr perpendicular to the superlattice plane as a function of modulation wavelength and these results are used to explain the anomalous behavior observed in the elastic properties of these materials. As compared to the other metallic superlattices we have studied (viz., Nb/Cu, Mo/Ni, and V/Ni), Au/Cr is the first to show a hardening.

I. INTRODUCTION

Over the past few years there have been a number of investigations of the elastic properties of superlattices. In almost all cases these properties were found to be anomalous since, contrary to expectation, they depend on the superlattice wavelength. A review of the experiments performed to date is given in Ref. 1 where the experimental results of Refs. 2–12 are conveniently summarized. The origin of the observed anomalies is not yet known. It has been proposed that electronic effects arising from the layering may be responsible for them but no quantitative calculations have been performed to date. A partial explanation was found[13] for the case of Mo/Ni superlattices by a fully relaxed molecular-dynamics calculation that reproduced the observed phonon softening in terms of the experimentally observed lattice expansion. However, an explanation for the lattice expansion in this system is not yet available.

Here, we report the results of a study of Au/Cr superlattices. This combination of elements, when in sandwich form, has been shown to have interesting properties[14,15] and the growth characteristics have also been described. The samples used here were fabricated under the same conditions as in Refs. 14 and 15 but many layers were built up to form a superlattice. The overall thickness of the superlattices is ~ 5000 Å with modulation wavelengths in the range of 30–600 Å. The ratio of thickness of the Au and Cr layers is 2:1 in all samples, and all are deposited on cleaved NaCl substrates.

This study is composed of two parts: the x-ray investigations, which are described in Sec. II, and the results of the Brillouin scattering results from surface waves which are presented in Sec. III. A discussion of the results is presented in Sec. IV, where a plausible explanation of the elastic anomalies is given on the basis of the x-ray results and the work of Ref. 13.

II. X-RAY DIFFRACTION MEASUREMENTS

The samples were fabricated by depositing the two components on a (100) surface of NaCl.[14,15] For each modulation period Λ, an alternate deposition was made of $\Lambda/3$ of Cr and $2\Lambda/3$ of Au as checked by thickness monitors. The conditions of growth are such that both elements have preferential growth along [100] directions of their respective cubic cells, i.e., body centered for Cr and face centered for Au. The two lattices are matched, in the sense that the atom positions and atomic density and symmetry of the (100) plane of Cr is almost identical to that of a (100) plane of Au rotated 45° in the plane (cf. Fig. 1). Evidence that the growth is indeed that shown in Fig. 1 is presented in Refs. 14 and 15. It is interesting to note that the lattice matching in the plane for this 45° geometry is almost perfect, i.e., $a_0(\mathrm{Au})/\sqrt{2}=2.8838$ Å and $a_0(\mathrm{Cr})=2.8839$. The most dramatic difference between Cr and Au layers is then the interatomic distance perpendicular to the layers: $d_{\mathrm{Au}} \cong \sqrt{2} d_{\mathrm{Cr}}$.

The purposes of our x-ray analysis are to verify the extent to which subsequent layers are coherent with each other to make a superlattice, to verify if indeed the chromium and gold are deposited with the expected crystallographic orientation, and if the interplanar distances are as in the bulk solid of each of the two species. In case of any unexpected results, it is necessary to check if this is due to interdiffusion, or is an intrinsic property of the superlattice.

Diffraction data were taken on samples with modulation periods between 30 and 150 Å (as measured by the thickness monitors) with a Rigaku spectrometer, which

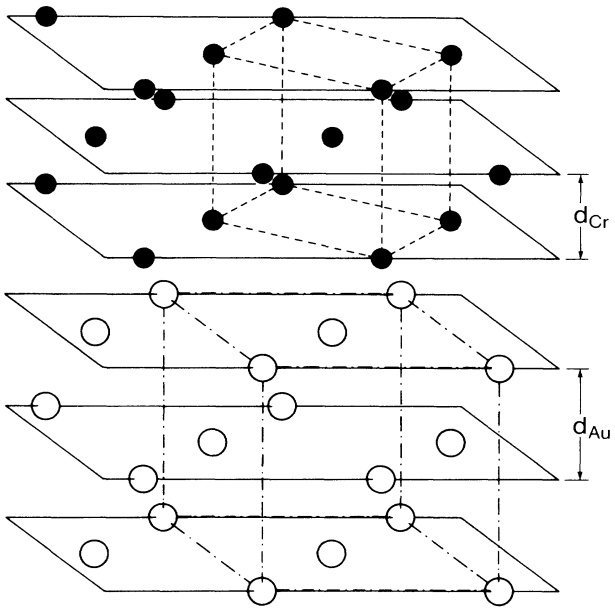

FIG. 1. The overlaying of bcc chromium (solid circles) on the fcc gold (open circles) lattice, in the [001] direction. $d_{Cr} \simeq d_{Au}/\sqrt{2}$.

utilized copper radiation and was equipped with a monochromator. Scans in the θ-2θ mode were made with the scattering vector normal to the surface of the films on the NaCl substrates, which has a typical area of a few tens of square millimeters. In this geometry the diffraction peaks provide information on the layering but not on the crystalline order within each layer. The alignment of this direction was obtained by rocking the crystals (ϕ motion) at a fixed detector angle 2θ. The width of the $(00l)$ lines was found to be $\Delta\phi \sim 1°$. The subsequent θ-2θ scans were made for an angle ϕ_0 corresponding to the intensity maximum. Measurements were taken from very small ($2\theta = 1°$) to large angles ($2\theta = 90°$). Although peaks are observed at small angles their intensities are unreliable because of small sample surface areas and the terraced character of the substrates. Furthermore, at large angles the intensities are very weak. Hence the measurements reported here are restricted to the range between the two very intense (200) and (400) lines from the NaCl substrate.

Figure 2 presents the (a) observed and (b) calculated intensities [multiplied by $\sin\theta \sin(2\theta)$] as a function of $2\sin\theta/\lambda$ for different modulation periods. Within each pattern the peaks appear at periodic intervals of $2\sin\theta/\lambda$, the minimum spacing being equal to $1/\Lambda$. The coherence of the superlattice is thus confirmed; and the periods Λ, as determined from the peak positions given in Table I and Fig. 3, are in excellent agreement with those measured by the thickness monitors during growth.

As can be observed in Fig. 2, the peaks with the highest intensities are clustered around the value of the reciprocal-lattice spacing of the (200) reflection of fcc gold, $1/d_{Au}$. A second, and considerably weaker group is clustered around the position approximately expected for the (200) reflection of bcc chromium $1/(d_{Cr})$. [Peaks just off scale on the right-hand side of Fig. 2(a) were masked by a very intense line from the NaCl substrate.] However, no particular line can be attributed to a typical gold lattice spacing, or to a chromium lattice distance: the individual line positions change dramatically with the modulation period, and so do their intensities. This behavior is not entirely unexpected and is a standard feature of the diffraction from superlattices. Assuming that the superlattice period is made up of an integral number of atomic planes, the intensities are given by

$$I(q) = \left| \sum_{m=1}^{M} f_m \exp(iqr_m) \right|^2 \delta(q - 2\pi n/\Lambda) , \tag{1}$$

where $q = 4\pi \sin\theta/\lambda$ is the scattering vector, f_m is the scattering amplitude of the plane at a distance r_m from the origin, and $\Lambda = M\bar{d}$, where M is the total number of atomic planes in the modulation period, $\bar{d}$ is the average interatomic distance, and n is a running integer. If the modulation period is made up to two slabs of different elements, each specified by a scattering amplitude, an interlayer spacing and a number of layers, the diffracted intensities take the form:[16]

$$I(q) = [A_1^2 + A_2^2 + 2A_1A_2\cos(\tfrac{1}{2}q\Lambda)]\delta(q - 2\pi n/\Lambda) \tag{2}$$

with

$$A_i = f_i \frac{\sin(qn_id_i/2)}{\sin(qd_i/2)} \tag{3}$$

and n_i is the number of atomic planes in a given layer. Equation (2) shows that the peaks occur simply at the positions assigned by the modulation period, whereas their intensities are entirely defined by the structure factors. If the two d spacings are sufficiently different, the interference term appearing in Eq. (2) becomes relatively small, and neglecting it in first order, the intensities for the two elements are clustered around their respective values of $1/d$, and are by far largest in the region included between the first zeros of the Airy function [Eq. (3)]: $q/2\pi = 1/d_i \pm 1/n_id_i$. In this approximation the "center of gravity" of each of the two clusters of peaks, labeled as due to gold and chromium, would provide the respective d spacings; the width of each cluster is inversely proportional to the layer thickness, and hence that of chromium should be roughly twice that of gold. Roughly speaking, this description is reproduced in the experimental pattern, which thus is consistent with that of a superlattice made of fcc gold and bcc chromium, each one deposited along a [001] direction.

The next issue is to determine more rigorously the interplanar spacings d_{Au}, d_{Cr}, and this can be obtained after examining more closely the line positions. In this analysis[17] we relax the (not proven) assumption that each period must contain an integral number of layers. Consider a series of lattice planes as long as an actual crystallite in the direction of the modulation. Each plane has a scattering power f_L and is at a distance r_L from an arbitrary origin. We can rewrite this distance as $r_L = L\bar{d} + \Delta_L$. The position of the Lth plane is thus redefined in terms of the displacement Δ_L from an ideal lattice with an interplanar spacing equal to the average spac-

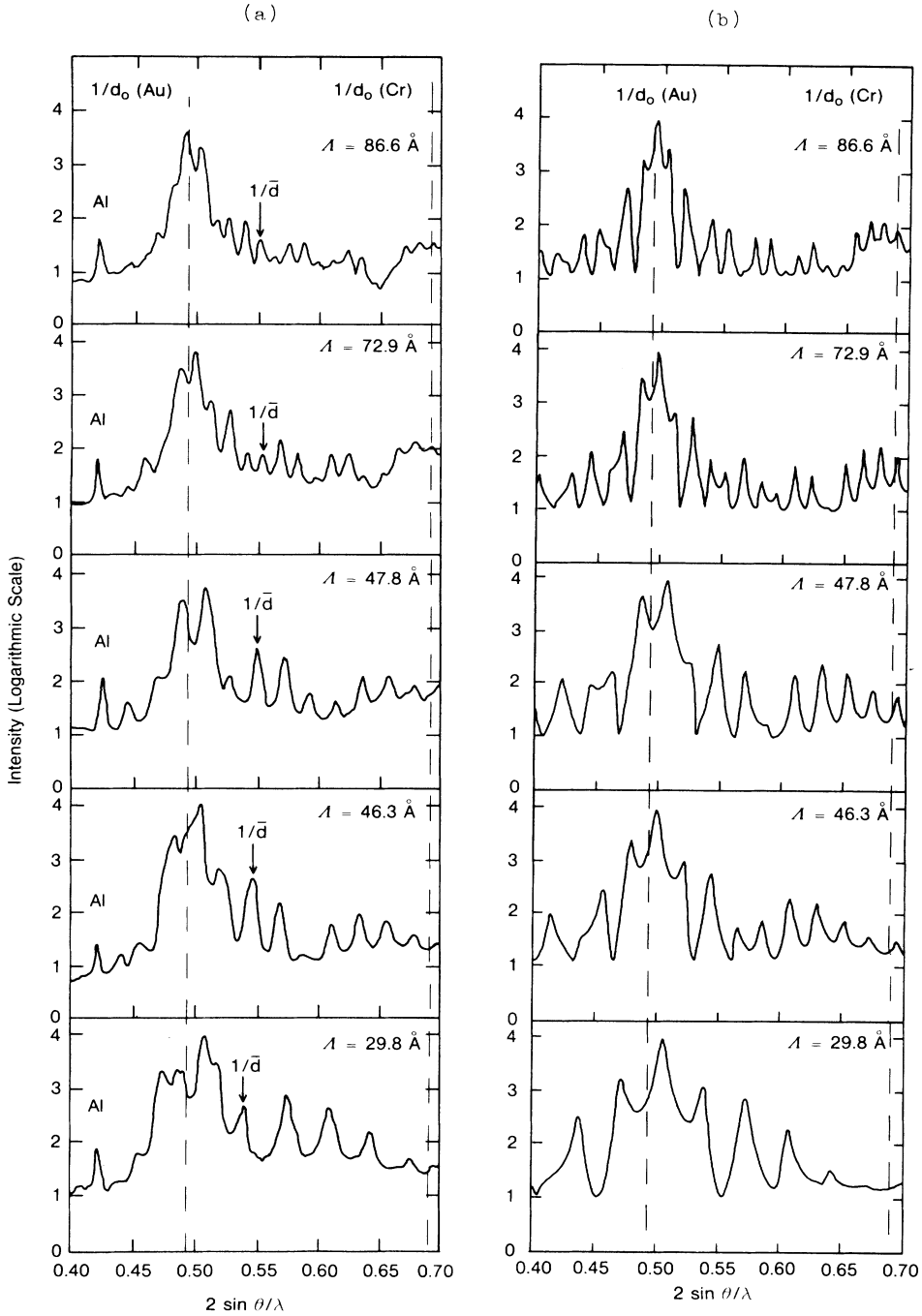

FIG. 2. (a) X-ray intensities [times $\sin\theta\sin(2\theta)$] measured in the reflection geometry for Au/Cr superlattices of different modulation periods, Λ, in the region of $2\sin\theta/\lambda$ between the (002) and the (004) peaks of the NaCl substrate. At the left of the spectrum an Al(111) line due to the sample holder is visible. (b) Calculated intensities for the various samples.

ing of the planes of the crystallite. (From these definitions, $\sum_L \Delta_L = 0$.) We can now define a mean effective scattering amplitude:

$$g = \frac{1}{N}\sum_L f_L \exp(iq\Delta_L) , \tag{4}$$

where N is the total number of layers. The fluctuations around this mean are then given by

$$\phi_L = f_L \exp(iq\Delta_L) - g . \tag{5}$$

The scattered intensities now can be written as

$$I = I_1 + I_2 = N^2 g^2 \delta(q - 2\pi/\bar{d}) + \sum_{L,L'} \phi_L \phi_{L'}^* \exp[iq(L - L')\bar{d}] . \tag{6}$$

TABLE I. $2\sin\theta/\lambda$ values of the diffraction peaks of Au/Cr superlattices. The two values given for Λ are determined by the thickness monitors (upper) and x-ray patterns (lower). For $\Lambda = 29.8$ Å, some lines (in parentheses) cannot be indexed.

Index \ Λ (Å)	90 86.6	75 72.9	51 47.8	45 46.3	30 29.8
−7	0.469	0.457			
−6	0.483				
−5	0.493	0.486	0.445	0.437	
−4	0.504	0.499	0.467	0.455	(0.485)
−3	0.518	0.511	0.487	0.480	(0.490)
−2	0.528	0.525	0.507	0.500	(0.517)
−1	0.540	0.540	0.526	0.520	0.507
0	0.553	0.553	0.548	0.543	0.539
1	0.563	0.567	0.570	0.565	0.574
2	0.575	0.581	0.591		0.608
3	0.587		0.612	0.609	0.641
4		0.609	0.633	0.631	0.674
5		0.222	0.654	0.653	
6	0.622		0.675	0.675	
7	0.634				
8		0.663			
9		0.677			
10	0.670	0.690			
11	0.681				
12	0.693				

The first term in Eq. (6) represents the diffraction peaks due to the average lattice spacing.

In order to specify the "disorder" scattering designated as I_2, we perform the sum over scattering planes displaced by $L-L'=R$:

$$\Phi_R = \sum_L \phi_L \phi^*_{L-R} , \tag{7}$$

and thus I_2 can be rewritten as

$$I_2 = \sum_R \Phi_R \exp(iqR\bar{d}) . \tag{8}$$

We now want to expand Φ_R in its Fourier components. In principle, the lowest wave vector to be chosen is equal to the reciprocal of the length of the crystallite; however, since we know that the strong perturbation from the average in the system is due to the modulation period Λ, we write simply

$$\Phi_R = \sum_p \Psi_p \exp(2\pi i p R\bar{d}/\Lambda) , \tag{9}$$

where Ψ_p is the amplitude of the pth Fourier component. The "disorder" scattering now takes the form:

$$I_2 = \sum_p \Psi_p \sum_R \exp[i(q+2\pi p/\Lambda)R\bar{d}] . \tag{10}$$

This is a set of Bragg reflections appearing at values of q:

$$q = \frac{2\pi n}{\bar{d}} - \frac{2\pi p}{\Lambda} , \tag{11}$$

where n,p are running integers. Hence for each Bragg peak due to the average $\bar{d}$ spacing (i.e., a fixed value of n) there is a set of lines, displaced from it at intervals of $2\pi/\Lambda$. This result, obtained for any noninteger number of atomic planes in the modulation period, is true irrespective of the deviation of the individual lattice spacing from the average. Observe, however, that in the treatment above we neglected the Fourier components larger than the modulation period Λ (imperfect modulation). The inclusion of these terms would cause a broadening of the peaks, which when added to that due to the finite size of the crystallite, might cause a merging of the peaks labeled with different p and n values [cf. Eq. (11)].

The identification of the $1/d$ ($p=0$) peak in the experimental pattern [Fig. 2(a)] is easily made, since the position

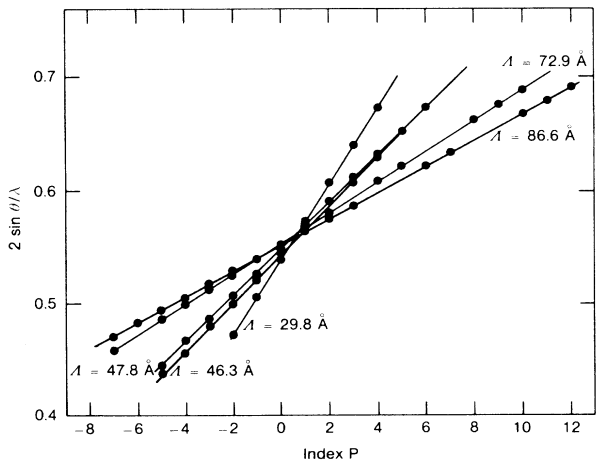

FIG. 3. The position of the diffraction peaks as a function of their index p.

of this peak should be close to the weighted average of the interplanar distance of the two constituents, especially in the superlattices with long modulation wavelengths, and should change smoothly when Λ is varied. The $1/\bar{d}$ peaks thus identified are marked by arrows in Fig. 2. All of the other peaks can thus be labeled in terms of a value of the index p, as is shown in Table I and in Fig. 3. As indicated graphically in Fig. 3, the peak positions are well described in terms of the modulation period Λ. (Omitted from the graph are a few peaks for the sample of shortest modulation period; these peaks, listed parenthetically in Table I, indicate the presence of a second phase in the sample.) The values of the $\bar{d}$ spacings thus obtained indicate that there is a gradual expansion of the average lattice when the modulation period is reduced. The knowledge of $\Lambda,\bar{d}$ from the diffraction data, and of the relative thickness of the two layers from the thickness monitors during deposition, give us the following set of equations:

$$\Lambda = n_{\mathrm{Au}} d_{\mathrm{Au}} + n_{\mathrm{Cr}} d_{\mathrm{Cr}} , \tag{12}$$

$$2 = (n_{\mathrm{Au}} d_{\mathrm{Au}})/(n_{\mathrm{Cr}} d_{\mathrm{Cr}}) , \tag{13}$$

$$\bar{d} = \Lambda/(n_{\mathrm{Au}} + n_{\mathrm{Cr}}) , \tag{14}$$

where now, consistent with the approach described above, the number of layers might be nonintegral. The full solution of these three equations with four unknowns requires the independent determination of one of the quantities. We have chosen to obtain a value for d_{Au} using the "center-of-gravity" method explained above, since gold is by far the strongest x-ray scatterer in the system. However, with these values of d_{Au}, the values of d_{Cr} derived with the aid of Eqs. (12)—(14) are unreasonable since d_{Cr} does not extrapolate to its bulk value for large Λ and the calculated intensities have little resemblance to the experimental ones.

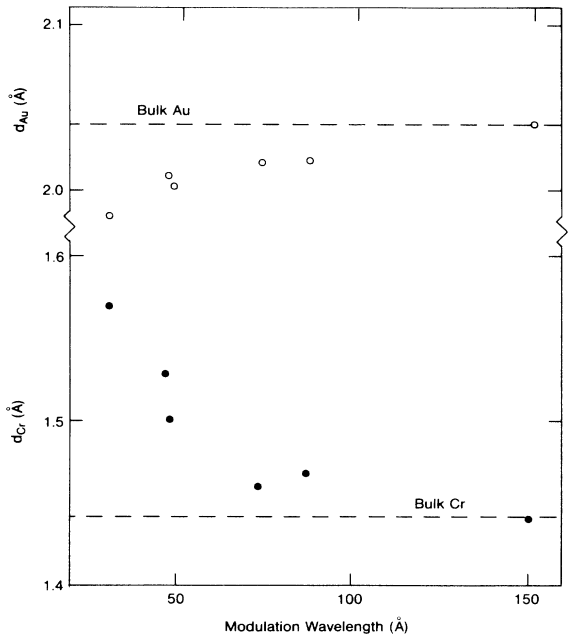

FIG. 4. The interplanar spacings of gold and chromium, as obtained by assuming that the distance of the gold and chromium planes at the interface is the same as d_{Au}.

An inherent hypothesis hidden in Eqs. (12)—(14) is that at the gold-chromium interface $d_{\mathrm{IF}} = (d_{\mathrm{Au}} + d_{\mathrm{Cr}})/2$. That this may not be the case can be argued by the fact that fcc alloys of chromium in gold have a lattice spacing very close to that of pure gold.[18] It therefore seems reasonable to take $d_{\mathrm{IF}} = d_{\mathrm{Au}}$, which produces some simple modifications to the expressions (12)—(14). In Fig. 4 we present the values of d_{Au} as determined by the center-of-gravity method and the values of d_{Cr} derived after assuming $d_{\mathrm{IF}} = d_{\mathrm{Au}}$. Included are the values of d_{Au} and d_{Cr} measured on a sample of a nominal modulation period of 150 Å—but for which the superlattice peaks were not resolved. Figure 2(b) presents the results of the intensities calculated numerically for a sequence of gold and chromium layers, each containing (in a random fashion) either n_i or $n_i + 1$ atomic planes, so that on the average the correct fractional value n_i derived from Eqs. (12)—(14) is obtained. In the calculation the coherence length was set at 50 layers, and a background contribution was added to facilitate comparison with experiment. As can be seen in Fig. 2(b) the calculated intensities show most of the basic features of the experimental patterns [Fig. 2(a)]. The discrepancies have to be attributed to the crudity of the model. We have assumed that the interfaces are perfect and, as a result, the zeros of the Airy function around $1/d_{\mathrm{Au}}$ are sharply defined. To smooth out the curves in Fig. 2(b) for closer agreement with experiment would require additional randomness in the plane stacking. Also, the calculation shows peaks larger than those observed for $q < 2\pi/d_{\mathrm{Au}}$; to obtain this asymmetry of intensities around $2\pi/d_{\mathrm{Au}}$ some interdiffusion of chromium in gold has to be invoked, as well as a gradual change of the lattice spacing within the gold layer. However, a further refinement of the model structure by a detailed least-squares fitting would not significantly alter the main conclusions obtained by very simple and direct methods, i.e., in these superlattices chromium retains the basic body-centered structure, but with an interplanar spacing stretched up to 8% along the [001] direction, while Au contracts slightly ($\sim 2\%$) along the growth direction. Given the excellent lattice matching between Au and Cr these changes cannot be attributed to strains at the interfaces.

III. ELASTIC MEASUREMENTS

The experimental setup used to perform Brillouin scattering from surface waves is described in Refs. 7, 10, and 12. In Fig. 5 we present our experimental results (crosses) for the surface wave velocity in the Au/Cr superlattices as a function of modulation wavelength. Since the phonon wavelengths probed in our experiments are ~ 3000 Å (i.e., much greater than Λ) the sound velocity is expected to be independent of Λ in this range.[19] However, as has been found in many other cases,[1–12] a large change is observed as Λ is varied. The behavior shown in Fig. 5 is different from that previously seen in Brillouin experiments on superlattices[7,10,12] as it is the first time that the velocity is found to increase as Λ is decreased from large

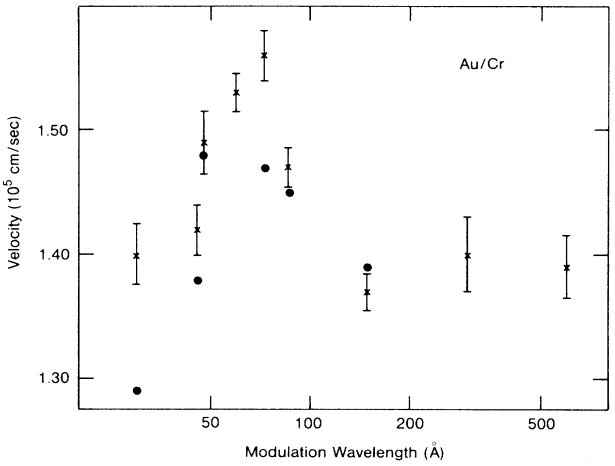

FIG. 5. Velocity of surface waves in Au/Cr superlattices as a function of modulation wavelengths. Crosses are experimental points and solid circles are calculated values as described in the text.

values. Furthermore, both an increase *and* a decrease are observed in a region of Λ values in which the x-ray studies show the existence of a superlattice.

The expected elastic constants of the superlattice can be calculated[20] in terms of the elastic constants of Au and Cr. However, since we are not dealing with a single crystal but with "crystallites" smaller than the wavelength of the phonons with preferential orientation along the [001] direction, it is not clear how the average of the elastic constants should be taken. In general terms, however, since the surface wave velocity in a superlattice material is dominated by the material with the softer elastic constants,[19,20] and since Au has shear constants much smaller than those of Cr, the measured velocity in superlattices with larger modulation wavelengths ($v=\sim 1.4$ km/sec) is close to that of pure Au ($v=1.2$–1.5 km/sec depending on the choice of elastic constants) with very little influence from the Cr ($v\cong 3.7$ km/sec). Based on this, we can conclude that the observed increase in surface wave velocity with decreasing Λ down to $\Lambda=72.9$ Å must be due to an effect occurring in the Au. A more quantitative analysis is given in the next section.

IV. DISCUSSION

The results presented here for the anomalous behavior of the sound velocity can be qualitatively interpreted as was done in Ref. 13 for the softening reported in Ref. 10 for Mo/Ni superlattices: viz., the lattice expansion (determined by x rays) accounts for a weakening of the interatomic bonding and a consequent reduction in the sound velocities. Here, for Au/Cr, the x-ray results indicate a progressive contraction of the Au lattice (as least perpendicular to the superlattice) and a large expansion of the Cr lattice as Λ is decreased. Hence, we would expect the elastic constants of Au to increase while those of Cr should decrease as Λ is decreased. Furthermore, since the elastic properties of the superlattice are dominated by the Au, we expect to see an increase in v as Λ is decreased. However, if the Cr were at some point to become softer than the Au, it would dominate the properties of the superlattice and a decrease in v would follow.

A full calculation of the changes in elastic properties of Au and Cr as a function of strain would be hampered by the uncertainties in a reliable potential for Cr. Nevertheless, the calculation of anharmonic effects of Ref. 13, and the qualitative arguments of the preceding paragraph, can be made somewhat more quantitative by the following simple analysis. It cannot be overemphasized, however, that what follows is only a plausibility argument and not a derivation. We start with the Murnaghan[21] equation of state which provides a relationship between the bulk modulus B and the density ρ, viz.,

$$B=B_0(\rho/\rho_0)^{B'} , \tag{15}$$

where B' is a constant that ranges between 4 and 7 for almost all materials. The generalization of this equation to other elastic moduli (C_{ij}) has been found to be a reasonable approximation for the case of H_2O at high pressures.[22] Also in the case of the layered compound GaS, Eq. (15) was written in the form[23]

$$C_{ij}=C_{ij}(0)\left[\frac{a_0}{a}\right]^{3B'} , \tag{16}$$

where a is the lattice spacing along the direction to which the C_{ij} refers, and it was found to adequately describe the behavior of C_{11} and C_{33} under pressure. Therefore, we shall take Eq. (16) to be valid also for shear elastic moduli and use it to describe the properties of Au/Cr superlattices.

The velocity of surface waves in our superlattices is given by

$$v=\beta\left[\frac{C_{44}(\text{eff})}{\bar{\rho}}\right]^{1/2} , \tag{17}$$

where $\bar{\rho}$ is the average density, β is a constant whose value is around 0.9, and C_{44}(eff) is an effective elastic constant of our superlattices. Using the expression from Ref. 20, we have

$$[C_{44}(\text{eff})]^{-1}=\tfrac{2}{3}[C_{44}(\text{Au})]^{-1}+\tfrac{1}{3}[C_{44}(\text{Cr})]^{-1} . \tag{18}$$

Combining Eqs. (16), (17), and (18) and using the lattice constants of Au and Cr from Fig. 4, we can estimate the changes in the surface wave velocity as a function of modulation wavelength. In doing this we have taken $\beta=0.94$, $\beta'=6$, $\bar{\rho}=15.3$ g/cm^3, and C_{44} as 2.50 and 10.0×10^{11} dyn/cm^2 for Au and Cr, respectively. The results of such a calculation for $\Lambda=30$–150 Å are shown in Fig. 5 as solid circles. We stress that the above procedure contains no fitting parameters except for B', and that can only be varied slightly. However, we have somewhat inconsistently chosen the value of C_{44} of Au to be that of a polycrystalline sample in order to produce better agreement with experiment: This can be justified to some extent by the fact that the sample is polycrystalline in the plane of the layers.

The general agreement between experiment and our simple approach to explain the hardening and the soften-

ing in Au/Cr superlattices, the fact that this approach also explains the softening in Mo/Ni and Nb/Cu superlattices,[24] and the fact that in Mo/Ni superlattices a full molecular dynamics calculation for the effects of strain on the elastic properties[13] produces quantitative agreement with experiment, seems to leave little doubt that the anomalous elastic properties are due to modifications of the lattice. However, the understanding of the elastic behavior in terms of the lattice modification still leaves the origin of the latter unexplained. Whether these are due to electron transfer from one material to the other, to quantization effects in the electronic energy levels of each layer, or simply to strains developed at the interfaces, this analysis shows how large these effects can be and how greatly the properties of thin films or layered materials may differ from those in the bulk form.

In the present case of Au/Cr superlattices, the expansion of the Cr lattice in the [001] direction as Λ decreases may be related to the observation of fcc Cr in Au/Cr/Au sandwich structures.[25] In that work, films having Cr thicknesses of 25 Å show diffraction features due to fcc Cr, but the corresponding extended x-ray-absorption fine-structure data are due to bcc Cr. Thus, it appears that metastable, fcc Cr may be formed in contact with Au. This tendency may be manifested in the present case by the $\leq 8\%$ stretch of the Cr lattice in the [001] direction, whereas fcc Cr would require a 41% stretch if no change occurred in the (100) plane.

V. CONCLUSIONS

We have studied superlattices of Au/Cr using x rays and Brillouin scattering. This is the first Brillouin investigation of a lattice-matched metallic superlattice and shows, contrary to previous studies on non-lattice-matched systems, the hardening of an elastic property. The elastic anomaly is explained in terms of the measured contraction of the Au and the concurrent expansion of the Cr lattice in the growth direction. Given the almost perfect matching of the Au and Cr lattice spacings, the measured expansion and contraction are difficult to explain as due to strains at the interfaces; no explanation is presently available to account for this behavior.

ACKNOWLEDGMENTS

One of us (G.P.F.) would like to thank Dr. P. R. Roach for enlightening discussions on the modeling of the superlattice structures. The assistance of C. H. Sowers is greatly appreciated. This work was supported by the U.S. Department of Energy, Basic Energy Science—Materials Sciences, under Contract No. W-31-109-ENG-38.

*Present address: Istituto di Struttura della Materia, Via Enrico Fermi 38 Frascati, Roma, Italy.

†Permanent address: Physics Department, Northern Illinois University, DeKalb, IL 60115.

[1]I. K. Schuller, *Institute of Electrical and Electronics Engineers 1985 Ultrasonics Symposium,* edited by B. R. McAvoy (IEEE, New York, 1985), p. 1093.

[2]V. S. Kysan and A. V. Lysenko, Fiz. Metal. Metalloved. **29**, 183 (1970).

[3]B. S. Berry and W. C. Pritchet, Thin Solid Films **33**, 19 (1976).

[4]W. M. C. Yang, T. Tsakalakos, and J. E. Hilliard, J. Appl. Phys. **48**, 876 (1977).

[5]L. R. Testardi, R. H. Willens, J. T. Krause, D. B. McWhan, and S. Nakahara, J. Appl. Phys. **52**, 510 (1981).

[6]H. Itozaki, Ph.D. thesis, Northwestern University, 1982 (unpublished).

[7]A. Kueny, M. Grimsditch, K. Miyano, I. Banerjee, C. M. Falco, and I. K. Schuller, Phys. Rev. Lett. **48**, 166 (1982).

[8]T. Tsakalakos and J. E. Hilliard, J. Appl. Phys. **54**, 734 (1983).

[9]G. E. Henein and J. E. Hilliard, J. Appl. Phys. **54**, 728 (1983).

[10]M. R. Khan, C. S. L. Chun, G. P. Felcher, M. Grimsditch, A. Kueny, C. M. Falco, and I. K. Schuller, Phys. Rev. B **27**, 7186 (1983).

[11]D. Baral, J. B. Ketterson, and J. E. Hilliard, J. Appl. Phys. **57**, 1076 (1985).

[12]R. Danner, R. P. Huebener, C. S. L. Chun, M. Grimsditch, and I. K. Schuller, Phys. Rev. B **33**, 3696 (1986).

[13]I. K. Schuller and A. Rahman, Phys. Rev. Lett. **50**, 1377 (1983).

[14]M. B. Brodsky, P. Marikar, R. J. Friddle, L. Singer, and C. H. Sowers, Solid State Commun. **42**, 675 (1982).

[15]M. B. Brodsky, L. R. Sill, and C. H. Sowers, J. Magn. Magn. Mater. **54-57**, 779 (1986); in *Layered Structures and Epitaxy,* Materials Research Society Symposium Proceedings, edited by J. M. Gibson, G. C. Osbourn, and R. M. Tromp (Materials Research Society, Pittsburg, 1986) Vol. 56, pp. 201—204.

[16]D. B. McWhan, in *Synthetic Modulated Structures,* edited by L. Chang and B. C. Giessen (Academic, New York, 1985).

[17]W. H. Zachariasen, *Theory of X-ray Diffraction in Crystals* (Wiley, New York, 1945).

[18]H. Okamoto and T. B. Massalski, Bull. Alloy Phase Diagrams **6**, 224 (1985).

[19]A. Kueny and M. Grimsditch, Phys. Rev. B **26**, 4699 (1982).

[20]M. Grimsditch, Phys. Rev. B **31**, 6818 (1985).

[21]F. D. Murnaghan, Proc. Nat. Acad. Sci. **30**, 244 (1944).

[22]A. Polian and M. Grimsditch, Phys. Rev. B **27**, 6409 (1983); Phys. Rev. Lett. **52**, 1312 (1984).

[23]A. Polian, J. M. Besson, M. Grimsditch, and H. Vogt, Phys. Rev. B **25**, 2767 (1982).

[24]I. K. Schuller and M. Grimsditch, J. Vac. Sci. Technol B **4**, 1444 (1986).

[25]S. M. Durbin, L. E. Berman, B. W. Batterman, M. B. Brodsky, and H. C. Hamaker (unpublished).